

# Testing of Quantum Gravity With Sub-Kilogram Acoustic Resonators

P. A. Bushev,<sup>1</sup> J. Bourhill,<sup>2</sup> M. Goryachev,<sup>2</sup> N. Kukharchyk,<sup>1</sup> E. Ivanov,<sup>2</sup> S. Galliou,<sup>3</sup> M. E. Tobar,<sup>2</sup> and S. Danilishin<sup>4</sup>

<sup>1</sup>*Experimentalphysik, Universität des Saarlandes, D-66123 Saarbrücken, Germany*

<sup>2</sup>*ARC Centre of Excellence for Engineered Quantum Systems,*

*University of Western Australia, Crawley, Western Australia 6009, Australia*

<sup>3</sup>*FEMTO-ST Institute, Université de Bourgogne Franche-Comté, CNRS, ENSMM, 25000 Besançon, France*

<sup>4</sup>*Institut für Theoretische Physik, Leibniz Universität Hannover and Max-Planck*

*Institut für Gravitationsphysik (Albert-Einstein-Institut), 30167 Hannover, Germany*

(Dated: July 19, 2022)

Recent progress in observing and manipulating mechanical oscillators at quantum regime provides new opportunities of studying fundamental physics, for example to search for low energy signatures of quantum gravity. For example, it was recently proposed that such devices can be used to test quantum gravity effects, by detecting the change in the  $[\hat{x}, \hat{p}]$  commutation relation that could result from quantum gravity corrections. We show that such a correction results in a dependence of a resonant frequency of a mechanical oscillator on its amplitude, which is known as amplitude-frequency effect. By implementing of this new method we measure amplitude-frequency effect for 0.3 kg ultra high-Q sapphire split-bar mechanical resonator and for  $\sim 10^{-5}$  kg quartz bulk acoustic wave resonator. Our experiments with sapphire resonator have established the upper limit on quantum gravity correction constant of  $\beta_0$  to not exceed  $5.2 \times 10^6$ , which is factor of 7 better than previously detected. The reasonable estimates of  $\beta_0$  from experiments with quartz resonators yields even more stringent limit of  $4 \times 10^4$ .

Historically, the development of quantum mechanics was driven largely by key experimental observations such as blackbody radiation, the photoelectric effect, and atomic spectra that were at complete odds with predictions made by the (classical) theoretical understanding of the time. At present, one of the grandest challenges of physics is to unite its two most successful theories: quantum mechanics (QM) and general relativity (GR), into a single unified mathematical framework. Attempting this unification has challenged theorists and mathematicians for several decades and numerous works have highlighted the seeming incompatibility between QM and GR [1]. In order to discover a successful theory for quantum gravity, experimental observations of quantum gravitational phenomena are required to guide the development of a mathematical framework in much the same way as experimental observations guided the development of quantum mechanics itself. It was generally supposed that this required energies at the Planck scale and therefore beyond the reach of current laboratory technology [2]. However in the relatively recent publication, I. Pikovsky et al. [3] proposed a new method of testing a set of quantum gravity (QG) theories [4–8] by using ingenuitive interferometric measurement of an optomechanical system. The prediction of most of the QG theories (such as, *e.g.*, string theory) and the physics of black holes lead to the existence of the minimum measurable length set by the Planck length  $L_p = \sqrt{\hbar G/c^3} \simeq 1.6 \times 10^{-35}$  m [4, 7, 8]. This results in the modification of the *Heisenberg uncertainty principle* (HUP) in such a way as to prohibit the coordinate uncertainty,  $\Delta x \sim \hbar/\Delta p$ , from tending to zero as  $\Delta p \rightarrow \infty$  [9–11]. The modified uncertainty relation, known as *generalised uncertainty principle* (GUP), is model-independent and can be written for a single de-

gree of freedom of a quantum system as:

$$\Delta x \Delta p \geq \frac{\hbar}{2} \left( 1 + \beta_0 \frac{\Delta p^2 + \langle p \rangle^2}{M_p^2 c^2} \right), \quad (1)$$

where  $\beta_0$  is a dimensionless model parameter,  $M_p = \sqrt{\hbar c/G} \simeq 2.2 \times 10^{-8}$  kg is Planck mass and  $\langle p \rangle$  is the quantum ensemble average of the momentum of the system. The dependence of minimum uncertainty of coordinate on average momentum reflects the connection of spacetime curvature and the density of energy and matter manifested in Einstein's equations of general relativity.

From the GUP (1) one can derive the new canonical commutation relation:

$$[\hat{x}, \hat{p}]_{\beta_0} = i\hbar \left[ 1 + \beta_0 \left( \frac{\hat{p}}{M_p c} \right)^2 \right], \quad (2)$$

that is deformed by the QG correction defined by the model parameter  $\beta_0$ . As shown by Kempf [6], parameter  $\beta_0$  defines the scale of the absolutely smallest coordinate uncertainty  $\Delta x_{min} = \hbar\sqrt{\beta_0}/(M_p c)$ . In this work, we experimentally set an upper limit on the value of the model parameter  $\beta_0$  using the dynamical implications of the contorted commutator on the oscillations of a high-Q mechanical resonator of mass  $m$  and (unperturbed) resonance frequency  $\Omega_0$ .

We start our consideration with the simple premise that the modification of the fundamental commutator for a harmonic oscillator, is equivalent to the nonlinear modification of the Hamiltonian by means of the perturbative transformation of momentum,  $\hat{p} \rightarrow \hat{p} - \beta_0 \hat{p}^3/(3M_p^2 c^2)$ , which restores the canonic commutator,  $[\hat{x}, \hat{p}] = i\hbar$ , at the expense of adding the non-linear term to the Hamiltonian of the resonator:  $\hat{H} \rightarrow \hat{H}_0 + \Delta\hat{H} = \left( \hat{p}^2/2m + \right.$

$m\Omega_0^2\hat{x}^2/2) + \beta_0\hat{p}^4/(3m(M_{pc})^2)$ . Such non-linear correction results in the dependence of the oscillator resonance frequency on its energy [6, 8]. The dynamics of the system can be described by a well known Duffing oscillator model characterized by amplitude dependence of the resonance frequency, i.e. so called amplitude-frequency effect [12, 13]. The necessary frequency resolution in order to sense subtle QG effects can be estimated by using the following expression:

$$\delta\Omega(A)/\Omega_0 = \beta_0(m_{\text{eff}}\Omega_0 A/M_{pc})^2, \quad (3)$$

where  $\delta\Omega = \Omega(A) - \Omega_0$  is the deviation of the amplitude-dependent resonance frequency  $\Omega(A)$  from the unperturbed value  $\Omega_0$ ,  $m_{\text{eff}}$  is the effective mass of the mode and  $A$  is the oscillation amplitude. So, the experimentally measured dependence of the resonance frequency on the amplitude, particularly its null result, may be used to set an upper limit for the model parameter  $\beta_0$ .

Other theories of QG predict another form of the GUP, *e.g.*, [7];

$$\Delta x \Delta p > \frac{\hbar}{2} \left[ 1 + \beta_0 \left( \frac{\Delta p}{M_{pc}} \right)^2 \right], \quad (4)$$

which depends only on the uncertainties of the canonical variables of the particle but not on their mean values. These theories can be tested by employing a different method of measuring the change of the oscillator ground-state energy  $E_{\text{min}}$  with respect to its unperturbed value  $\hbar\Omega_0/2$  [14]. In such tests, QG manifests in increased uncertainty of momentum and it yields higher minimal energy. The lowest modal energies measured in large mechanical systems such as AURIGA detector with effective mass of the mode  $m_{\text{eff}} \simeq 1000$  kg [14] and in dumbbell sapphire oscillator with  $m_{\text{eff}} \simeq 0.3$  kg [15] set the limit on the QG model parameter  $\beta_0 \lesssim 3 \times 10^{33}$ , which is still too large compared to the predicted values of the order of unity [16].

The above mentioned theoretical considerations do not specify, which degree of freedom is subject to the QG corrections. If one considers a center of mass mode, then the scale of perturbation is strongly enhanced for the heavier than the Planck mass oscillators, as compared to individual atoms and molecules in the lattice. For instance, the precise measurement of the Lamb shift in hydrogen yielded an upper bound for the model parameter  $\beta_0 < 10^{36}$  [16]. Although, the recent experiments with microscopic high-Q oscillators with effective masses ranging from  $10^{-11}$  kg to  $10^{-5}$  kg, established the new upper bound for  $\beta_0 < 3 \times 10^7$  [13]. The intrinsic acoustic non-linearity of micro oscillators prevented to test quantum gravity corrections with the greater precision.

Thus, the frequency-stable, high-Q oscillator with  $m_{\text{eff}} \gg M_p$  and small intrinsic acoustic nonlinearity turns

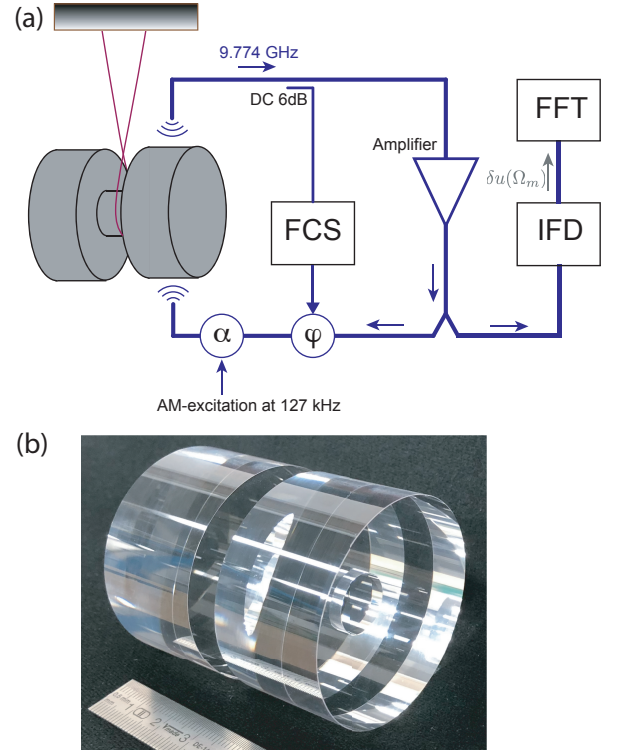


FIG. 1: (Color online) (a) Simplified schematic diagram of the experimental setup. Mechanical motion of the SB resonator results in frequency modulation of the microwave sapphire loop oscillator. The FCS stands for the frequency control system which actuates the phase of the microwave signal by means of voltage-controlled phase shifter  $\varphi$ . The DC is the directional coupler. Approximately a half of the generated power is directed to the interferometric frequency discriminator (IFD), which converts frequency fluctuation of the microwave signal into synchronous fluctuations of the output voltage. The output signal  $\delta u(\Omega_m)$  is analyzed with FFT spectrum analyzer. For the excitation of the mechanical motion, the amplitude of the microwave oscillator is modulated at the mechanical resonance frequency by using voltage controlled attenuator  $\alpha$ . (b) Picture of the sapphire SB resonator. The ruler shows the scale of the system.

out to be the best system for probing the deformed commutator described by Eq. (2). In the following we describe an experiment with the sub-kilogram split-bar (SB) sapphire mechanical oscillator, where we demonstrate improvement for the upper value of the correction parameter  $\beta_0$  compared to the previous work with intermediate range mechanical oscillators [13] by nearly an order of magnitude. In addition to that, we provide the reasonable estimates of  $\beta_0$  from experiments with bulk acoustic wave (BAW) quartz resonators yields even more stringent limit of  $4 \times 10^4$ .

Microwave oscillators based on electromagnetic Whispering Gallery Mode (WGM) sapphire crystals offer excellent short- and middle-term frequency stability [17] due WGM high quality factors exceeding  $10^8$  and ex-

istence of frequency-temperature turnover points. For these reasons these devices found applications in fundamental tests [18–20]. The mechanical modes of sapphire resonators may attain  $Q_M \simeq 10^8 - 10^9$  [21–23]. The resonance frequencies of WGMs are very sensitive to changes in circumference, height of the cylinder resonator and to strain in the crystal lattice thus yielding the necessary coupling between mechanical and electromagnetic degrees of freedom for the observation of mechanical motion. Yet, no acoustic nonlinearities have been detected for the large sapphire mechanical resonators making these devices an excellent platform for QG tests.

The experimental setup, shown in Fig. 1(a), is based on a cylindrical dumbbell shape or split-bar (SB) sapphire resonator, which is fabricated out of a single crystal HEMEX-grade sapphire fabricated by GT Advanced Technologies Inc., USA. The rotation symmetry axis of the resonator is parallel to the c-axis of the crystal. The SB resonator consists of two bars with diameter 55 mm and height 28 mm, which are separated by the neck of diameter 15 mm and length 8 mm, see Fig. 1(b). Two electromagnetic WGM resonators are formed in each bars and undergo the same mechanical motion, i.e. they oscillate in phase for the breathing mode, which is similar to the fundamental longitudinal mode of the conventional cylindrical resonator of the same length and diameter. The resonance frequency of this mode is  $\Omega_0/2\pi = 127.071$  kHz and its effective mass is calculated by using finite element modelling  $m_{\text{eff}} = 0.3$  kg. In order to maximize mechanical Q-factor, the resonator is suspended via a niobium wire-loop around the neck. The whole construction is placed inside temperature stabilized vacuum chamber at 300 K. The vacuum chamber in turn is placed on vibration isolation platform and kept at a pressure of  $\sim 10^{-2}$  mBar.

A parametric transducer is used to detect the mechanical vibrations of the SB resonator, see ref. [15] for the details. For that purpose, the WGM sapphire resonator serves as a dispersive element inside a closed electronic loop, which together with an amplifier and a phase shifter constitute a microwave oscillator operating at the resonance frequency of the chosen WGM mode [24]. An interferometric frequency control system (FCS) suppresses spurious frequency fluctuations and locks the microwave oscillator to the frequency of the  $\text{WGE}_{15,1,1}$  mode at  $\omega_{\text{WGE}}/2\pi \simeq 9.774$  GHz [25]. The in-loop voltage-controlled attenuator  $\alpha$  is used for the parametric excitation of the mechanical vibrations at 127 kHz.

Approximately a half of the generated power inside the microwave sapphire oscillator is diverted to the interferometric frequency discriminator (IFD). The IFD contains microwave interferometer with actively controlled balance in order to deal with frequency variations and changes of ambient temperature. The output signal of IFD is a linear function of its input frequency and is

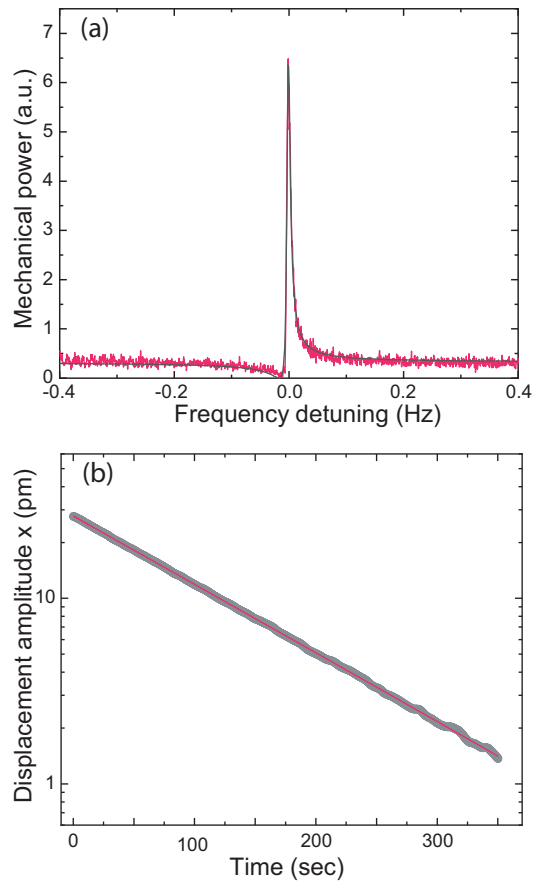


FIG. 2: (Color online) (a) Mechanical response of the SB resonator to the acoustic excitation of the in-phase breathing mode around  $\Omega_0/2\pi = 127070.9695$  Hz. The solid curve shows the fit to the quadrature signal due to double-balanced mixing. (b) Typical ringdown measurement of the in-phase breathing mode. The solid curve shows the fit to the exponential decay corresponding to the mechanical  $Q_M = 3.4 \cdot 10^7$ .

measured with HP 89410A spectrum analyzer. All instruments are time referenced to the hydrogen maser frequency standard VCH-103. Due to the low phase noise of the oscillator, the calibrated displacement noise floor achievable with the developed setup is measured to be  $\delta x \simeq 4 \times 10^{-15}$  m/ $\sqrt{\text{Hz}}$ .

The spatial overlap between microwave and mechanical modes results in the interaction between these degrees of freedom, which can be described by the standard opto-mechanical Hamiltonian  $\hat{H}_{\text{int}} = -\hbar g_0 \hat{a}^\dagger \hat{a} \hat{x}$ , where  $g_0$  is a single photon opto-mechanical coupling,  $\hat{a}^\dagger, \hat{a}$  are raising and lowering operators for the WGM and  $\hat{x}$  is canonical position operator for the center of mass mechanical motion [26]. The microwave signal modulated at the resonance frequency of mechanical mode  $\Omega_0$  induces radiation-pressure force which drives mechanical vibrations. The calibration of amplitude of center of mass motion is made by using the standard expression

$$\delta u(\Omega) = \delta x(\Omega) (du/df) (df/dx), \quad (5)$$

where  $df/dx$  is determined from the amplitude of the output IFD signal  $\delta u(\Omega)$ . That signal is proportional to the applied modulated power  $\delta P$

$$\delta u(\Omega) = \chi \left( \frac{du}{df} \right) \left( \frac{df}{dx} \right)^2 \delta P, \quad (6)$$

where  $\chi$  is the constant describing electromagnetic coupling of the signal and mechanical property of the oscillator [15]. The transduction constant is calculated to be  $\delta x/\delta u = 526 \text{ nm/mV}$ .

The mechanical response of the SB-resonator to the acoustic excitation in the vicinity of the resonance frequency is shown in Fig. 2(a). The applied excitation signal at 127 kHz is relatively weak resulting in the maximal amplitude of mechanical vibrations of 6 pm. The output signal is measured by using phase-sensitive interferometric setup which results in superposition of dispersive and absorptive quadrature components. The solid curve displays the fit of the experimental data to such composite absorptive-dispersive response and yields the resonance frequency of the mechanical resonator  $\Omega_0/2\pi = 127070.9695 \pm 0.0003 \text{ Hz}$ , its FWHM linewidth  $\Gamma_M/2\pi = 3.5 \text{ mHz}$  and the  $55^\circ$  degrees mismatch between the arms of the IFD.

The ringdown measurements of the mechanical vibrations are made in two steps. In the first step the resonance frequency of mechanical vibrations  $\Omega_0/2\pi$  is determined. For that purpose, the radiation pressure force is applied to the resonator for the time sufficient to settle the mechanical vibrations (several minutes). Then, the output signal  $\delta u(\Omega)$  is measured for every frequency point in the scanning range of 1 Hz. The resonance frequency corresponds to the point which yields the maximal IFD response  $\delta u(\Omega)$ . This procedure is repeated for the different excitation amplitudes (20-35 pm) in every single experimental run and detected no resonance frequency shift within accuracy of 10 mHz determined by the resolution bandwidth of FFT analyzer. In the second step, after the mechanical resonance frequency is located, the AM-excitation is turned off, and then the mechanical vibrations are measured as they decrease due to acoustic losses. The amplitude and frequency of the decaying vibrations, i.e. the amplitude and the frequency of the spectral peak, is then tracked and recorded every 0.2 s. For that purpose a marker is placed on the maximum voltage value in the spectra, and its frequency and amplitude is recorded for every time bin. The frequency accuracy of such measurements is determined by the resolution bandwidth of the FFT analyzer, which is set to 5 Hz.

The typical ringdown measurement is presented in Fig. 2(b). For this particular example, the resonant frequency is  $\Omega_0/2\pi = 127070.97 \text{ Hz}$ . The solid curve shows the fit of the experimental data to the exponential decay with characteristic time constant  $\tau = 173 \text{ sec}$  which yields the mechanical quality factor  $Q_M = \Omega_0\tau/2 =$

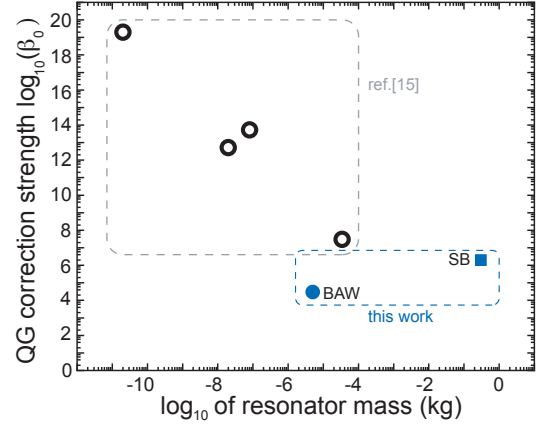


FIG. 3: (Color online) The correction strength  $\beta_0$  versus mass of mechanical oscillator determined in various experiments. The open circles reports its upper limit obtained by measuring the amplitude-frequency effect of microscopic high-Q resonators with resonance frequencies lying in kHz range [13]. The closed circle is the estimated  $\beta_0$  for the quartz BAW at LD-cut, see ref. [12]. The square is the upper limit for  $\beta_0$  obtained in this work with sapphire split-bar resonator.

$3.4 \cdot 10^7$  and the same FWHM linewidth  $\Gamma_M$  which is found in mechanical response measurements. In addition to the extracting of the parameters of the exponential decay, the Duffing equation was numerically solved in order to attain the best fit parameters for the ringdown amplitudes. Following this procedure we extract the upper limit for the QG model parameter to be  $\beta_0 < 6 \times 10^{11}$ .

The frequency measurements yield much more stringent limit on  $\beta_0$ . In all measured ringdown series, there is no evidence of any detectable frequency shift up to the maximum amplitude of mechanical displacement of 75 pm. The null-frequency shift measured in the experiment corresponds to the accuracy of  $\delta\Omega/\Omega_0 = 3.9 \times 10^{-5}$  and accordingly to the Eq. 3 yields the upper limit for the QG model parameter  $\beta_0 < 5.2 \times 10^6$ .

The sapphire SB resonator demonstrate a large potential for even more stringent test of  $\beta_0 < 1$ . Here, we propose two possible ways to improve the experiment. Firstly, the mechanical response (Fig. 2(a)) could be measured for much larger input power  $\delta P$ . It is possible to excite vibrations in sapphire resonator with amplitude of several nanometers [23]. That would result is much higher signal-to-noise ratio and as a consequence would improve the accuracy of determination of the mechanical resonance frequency  $\Omega_0$  to be better than 1 mHz. Together with an increase of the oscillation amplitude by two-three orders of magnitude that may result in  $10^7$  fold improvement for the upper limit on  $\beta_0$ . Secondly, one can implement an electromechanical sapphire oscillator by closing a feedback loop with the IFD output signal  $\delta u(\Omega_M)$ . In that case the uncertainty in determination of frequency shift will be decreased with the integration time  $T$  as  $1/\sqrt{\Omega_0 T}$ . Assuming the driving amplitude of

SB resonator of  $A \simeq 1$  nm and average time of  $T = 1$  hour, the testable limit  $\beta_0 \simeq 1$  is within experimental accuracy.

Another mechanical system, namely quartz bulk BAW resonator also constitutes a fruitful platform for precise tests of quantum gravity. This system exhibits high resonance frequency  $\Omega_0/2\pi \simeq 10$  MHz, milligram scale of the effective mass of oscillating modes [27], large Q-factor close to  $10^{10}$  at low temperatures [28] and high frequency stability of electromechanical oscillators reaching the level of  $5 \times 10^{-14}$ . The above listed features of quartz BAW are very attractive for fundamental tests such as Lorentz symmetry [29]. However, we note that quartz crystals possess its own quite strong elastic non-linearities that can mimic the quantum gravity effect. These non-linearities lead to a similar frequency shift, quadratic in amplitude and known as amplitude-frequency effect or isochronism, see ref. [30], p. 245. This effect can be made to nearly vanish by means of an optimal choice of the cut angle of the crystal, known as LD-cut [12, 31]. The QG correction strength can be estimated from Eq. 3 and by using the experimental parameters  $m_{\text{eff}} = 5$  mg,  $\Omega_0/2\pi = 10$  MHz,  $\delta\Omega/2\pi \simeq 1$  mHz,  $A \simeq 1$  nm. Our estimation yields  $\beta_0 \lesssim 4 \times 10^4$ , which is still limited by elastic non-linearity. In order to single out quantum gravity frequency from such non-linearity, the amplitude frequency shift shall be measured in dependence on the effective mass of the resonating mode. We also believe that experimenting with kilogram scale quartz BAW [32] will result in much more stringent test of the quantum gravity model parameter in regime  $\beta_0 \lesssim 1$ , because of weaker non-linearity due to the lower acoustic energy density and much larger effective mass.

To conclude, we have presented measurement of the upper limit on QG correction strength by using ultrahigh-Q mechanical sapphire resonator with sub-kilogram mass of the resonating mode. In the original work [3], a light pulse is proposed to reflect off an oscillator four times, separated by one quarter the oscillation period - before having the its phase measured. Our analysis and experiment shows, that one can attain the same goal in continuous RF measurement, which makes the experiment much simpler and reliable because the oscillation frequency can be measured with more precision compared to any other physical parameter. The overview of results of testing  $\beta_0$  with mechanical oscillators is presented in Fig. 3, which shows the measured constraints on the QG correction strength in dependence of the effective mass of the mechanical resonator. The heavier oscillators allows for the better determination of the correction strength. The remarkable high-Q and frequency stability of state of the art quartz BAW resonators and SB sapphire resonator in conjunction with low acoustic non-linearities have a great potential for its further applications in precise tests of minimal length scale scenarios for the quantum gravity theories [33].

- 
- [1] S. Hossenfelder, *Experimental Search for Quantum Gravity* (Springer, Cham, 2018).
  - [2] G. Amelino-Camelia, *Nature* **410**, 1065 (2001).
  - [3] I. Pikovski, M. R. Vanner, M. Aspelmeyer, M. S. Kim, and C. Brukner, *Nat. Physics* **8**, 393 (2012).
  - [4] M. Maggiore, *Phys. Lett. B* **304**, 65 (1993).
  - [5] M. Maggiore, *Phys. Rev. D* **49**, 5182 (1994).
  - [6] A. Kempf, G. Mangano, and R. B. Mann, *Phys. Rev. D* **52**, 1108 (1995).
  - [7] L. J. Garay, *Int. J. Mod. Phys. A* **10**, 145 (1995).
  - [8] A. F. Ali, S. Das, and E. C. Vagenas, *Phys. Rev. D* **84**, 044013 (2009).
  - [9] S. W. Hawking, *Nuc. Phys. B* **144**, 349 (1978).
  - [10] G. Amelino-Camelia, *Phys. Rev. D* **62**, 024015 (2000).
  - [11] Y. J. Ng and H. van Dam, *Found. Phys.* **30**, 795 (2000).
  - [12] N. Gufflet, F. Sthali, J.-J. Boy, R. Bourquin, and M. Mourey, *IEEE Trans. Ultrasonics, Ferroelectrics, and Frequency Control* **48**, 1681 (2001).
  - [13] M. Bawaj, C. Biancofiore, M. Bonaldi, F. Bonfigli, A. Borrielli, G. D. Giuseppe, L. Marino, R. Natali, A. Pontin, G. A. Prodi, et al., *Nature Comm.* **6**, 7503 (2015).
  - [14] F. Marin, F. Marino, M. Bonaldi, M. Cerdonio, L. Conti, P. Falferi, R. Mezzena, A. Ortolan, G. A. Prodi, L. Taffarello, et al., *Nat. Physics* **9**, 71 (2012).
  - [15] J. Bourhill, E. Ivanov, and M. E. Tobar, *Phys. Rev. A* **92**, 023817 (2015).
  - [16] S. Das and E. C. Vagenas, *Phys. Rev. Lett.* **101**, 221301 (2008).
  - [17] E. N. Ivanov and M. E. Tobar, *IEEE Transactions on Ultrasonics, Ferroelectrics, and Frequency Control* **56**, 263 (2009).
  - [18] P. L. Stanwix, M. E. Tobar, P. Wolf, C. R. Locke, and E. N. Ivanov, *Phys. Rev. D* **74**, 081101 (2006).
  - [19] V. Giordano, S. Grop, B. Dubois, P.-Y. Bourgeois, Y. Kersal, G. Haye, V. Dolgovskiy, N. Bucalovic, G. Di Domenico, S. Schilt, et al., *Review of Scientific Instruments* **83**, 085113 (2012).
  - [20] M. Nagel, S. Parker, E. Kovalchuck, P. Stanwix, J. Hartnett, E. Ivanov, A. Peters, and M. Tobar, *Nature Comm.* **6**, 8174 (2015).
  - [21] V. B. Braginsky, V. P. Mitrofanov, and V. I. Ivanov, *Systems with small dissipation* (The University of Chicago Press, Chicago, 1985).
  - [22] M. Tobar, E. Ivanov, D. Oi, B. Cuthbertson, and D. Blair, *Appl. Phys. B* **64**, 153 (1997).
  - [23] C. R. Locke, M. E. Tobar, and E. N. Ivanov, *Rev. Sci. Instruments* **71**, 2732 (2000).
  - [24] D. B. Leeson, *Proc. IEEE* **56**, 329 (1966).
  - [25] E. N. Ivanov, M. E. Tobar, and R. A. Woode, *IEEE Transactions on Ultrasonics, Ferroelectrics, and Frequency Control* **45**, 1526 (1998).
  - [26] M. Aspelmeyer, T. J. Kippenberg, and F. Marquardt, *Rev. Mod. Phys.* **86**, 1391 (2014).
  - [27] J. Bon, L. Neuhaus, S. Deléglise, T. Briant, P. Abbé, P. Cohadon, and S. Galiou, *J. Appl. Phys.* **124**, 073104 (2018).
  - [28] M. Goryachev, D. L. Creedon, S. Galiou, and M. E. Tobar, *Phys. Rev. Lett.* **111**, 085502 (2013).
  - [29] A. Lo, P. Haslinger, E. Mizrachi, L. Anderegg, H. Müller, M. Hohensee, M. Goryachev, and M. E. Tobar, *Phys.*

- Rev. X **6**, 011018 (2016).
- [30] W. P. Manson and R. N. Thurston, *Physical Acoustics: principles and methods vol. XI* (Academic Press, New York, 1975).
  - [31] S. Galliou, F. Sthali, J. Boy, R. Bourquin, and M. Mourey, 2004 IEEE International Ultrasonics, Ferroelectrics, and Frequency Control Joint 50th Anniversary Conference p. 475 (2004).
  - [32] J. Vig and D. Howe, IEEE Transactions on Ultrasonics, Ferroelectrics, and Frequency Control **60**, 428 (2013).
  - [33] S. Hossenfelder, Living Rev. Relativity **16**, 2 (2013).